

Discovery of extremely halophilic, methyl-reducing euryarchaea provides insights into the evolutionary origin of methanogenesis

Sorokin, Dmitry Y.; Makarova, Kira S.; Abbas, Ben; Ferrer, Manuel; Golyshin, Peter N.; Galinski, Erwin A.; Ciordia, Sergio; Mena, María Carmen; Merkel, Alexander Y.; Wolf, Yuri I.

DOI

[10.1038/nmicrobiol.2017.81](https://doi.org/10.1038/nmicrobiol.2017.81)

Publication date

2017

Document Version

Accepted author manuscript

Published in

Nature Reviews. Microbiology

Citation (APA)

Sorokin, D. Y., Makarova, K. S., Abbas, B., Ferrer, M., Golyshin, P. N., Galinski, E. A., Ciordia, S., Mena, M. C., Merkel, A. Y., Wolf, Y. I., Van Loosdrecht, M. C. M., & Koonin, E. V. (2017). Discovery of extremely halophilic, methyl-reducing euryarchaea provides insights into the evolutionary origin of methanogenesis. *Nature Reviews. Microbiology*, 2(8), Article 17081. <https://doi.org/10.1038/nmicrobiol.2017.81>

Important note

To cite this publication, please use the final published version (if applicable).
Please check the document version above.

Copyright

Other than for strictly personal use, it is not permitted to download, forward or distribute the text or part of it, without the consent of the author(s) and/or copyright holder(s), unless the work is under an open content license such as Creative Commons.

Takedown policy

Please contact us and provide details if you believe this document breaches copyrights.
We will remove access to the work immediately and investigate your claim.

1 **Discovery of extreme halo(alkali)philic, thermophilic, methyl-reducing**
2 **methanogenic euryarchaea**

3
4 Dimitry Y. Sorokin^{1,2*}, Kira S. Makarova³, Ben Abbas², Manuel Ferrer⁴, Peter N. Golyshin⁵,
5 Erwin A. Galinski⁶, Sergio Ciordia⁷, María Carmen Mena⁷, Alexander Y. Merkel¹, Yuri I.
6 Wolf³, Mark C.M. van Loosdrecht², Eugene V. Koonin^{3*}

7
8 ¹*Winogradsky Institute of Microbiology, Centre for Biotechnology, Russian Academy of Sciences, Moscow,*
9 *Russia;*

10 ²*Department of Biotechnology, Delft University of Technology, Delft, The Netherlands;*

11 ³*National Center for Biotechnology Information, National Library of Medicine, National Institutes of Health,*
12 *Bethesda, MD, USA;*

13 ⁴*Institute of Catalysis, CSIC, Madrid, Spain;*

14 ⁵*School of Biological Sciences, Bangor University, Gwynedd, UK*

15 ⁶*Institute of Microbiology and Biotechnology, Rheinische Friedrich-Wilhelms University, Bonn, Germany*

16 ⁷*Proteomics Facility, Centro Nacional de Biotecnología, CSIC, Madrid, Spain*

17
18
19 *Corresponding authors:

20 Dimitry Y. Sorokin: soroc@inmi.ru; d.sorokin@tudelft.nl

21 Eugene V. Koonin: koonin@ncbi.nlm.nih.gov

22

23 Methanogenic archaea are major players in the global carbon cycle and in the biotechnology of
24 anaerobic digestion. The phylum *Euryarchaeota* includes diverse groups of methanogens that are
25 interspersed with non-methanogenic lineages. So far methanogens inhabiting hypersaline
26 environments have been identified only within the order *Methanosarcinales*. We report the
27 discovery of a deep phylogenetic lineage of extremophilic methanogens in hypersaline lakes, and
28 present analysis of two nearly complete genomes from this group. Within the phylum
29 *Euryarchaeota*, these isolates form a separate, class-level lineage "Methanonatronarchaeia" that
30 is most closely related to the class *Halobacteria*. Similar to the *Halobacteria*,
31 "Methanonatronarchaeia" are extremely halophilic and do not accumulate organic
32 osmoprotectants. These methanogens are heterotrophic methyl-reducers that utilize C₁-
33 methylated compounds as electron acceptors and formate or hydrogen as electron donors. The
34 genomes contain an incomplete and apparently inactivated set of genes encoding the upper
35 branch of methyl group oxidation to CO₂ and membrane-bound heterosulfide reductase and
36 cytochromes. These features differentiates "Methanonatronarchaeia" from all known methyl-
37 reducing methanogens. The high intracellular concentration of potassium implies that
38 "Methanonatronarchaeia" employ the "salt-in" osmoprotection strategy. The discovery of
39 extremely halophilic, methyl-reducing methanogens related to haloarchaea sheds new light on
40 the origin of methanogenesis and shows that the strategies employed by methanogens to thrive in
41 salt-saturating conditions are not limited to the classical methylotrophic pathway.

42 **Introduction**

43

44 Methanogenesis is one of the key terminal anaerobic processes of the biogeochemical carbon
45 cycle both in natural ecosystems and in industrial biogas production plants ^{1,2}. Biomethane is a major
46 contributor to global warming ³. Methanogens comprise four classes, "*Methanomicrobia*",
47 *Methanobacteria*, *Methanopyri* and *Methanococci*, and part of the class *Thermoplasmata*, within the
48 archaeal phylum *Euryarchaeota*⁴⁻⁷. The recent metagenomic discovery of putative methyl-reducing
49 methanogens in the Candidate phyla "*Bathyarchaeota*" ⁸ and "*Verstaraetearchaeota*" ⁹ indicates that
50 methanogenesis might not be limited to *Euryarchaeota*.

51 Three major pathways of methanogenesis are known^{1,2}: hydrogenotrophic (H₂, formate and
52 CO₂/bicarbonate as electron acceptor), methylotrophic (dismutation of C₁ methylated compounds to
53 methane and CO₂) and acetoclastic (disruption of acetate into methane and CO₂). In the
54 hydrogenotrophic pathway, methane is produced by sequential 6-step reduction of CO₂. In the
55 methylotrophic pathway, methylated C₁ compounds, including methanol, methylamines and
56 methylsulfides, are first activated by specific methyltransferases. Next, one out of four methyl groups
57 is oxidized through the same reactions as in the hydrogenotrophic pathway occurring in reverse, and
58 the remaining three groups are reduced to methane. In the acetoclastic pathway, methane is produced
59 from the methyl group after activation of acetate. The only enzyme that is uniquely present in all three
60 types of methanogens is methyl-CoM reductase, a Ni-corrinoid protein catalyzing the last step of
61 methyl group reduction to methane ¹⁰⁻¹².

62 The recent discovery of methanogens among *Thermoplasmata* ^{5,13-15} drew attention to the
63 fourth, methyl-reducing, pathway, previously characterized in *Methanosphaera stadtmanae*
64 (*Methanobacteria*) and *Methanomicrococcus blatticola* ("*Methanomicrobia*") ¹⁶⁻²⁰. In this pathway, C₁
65 methylated compounds are used only as electron acceptors, whereas H₂ serves as electron donor. In the
66 few known representatives, the genes for methyl group oxidation to CO₂ are either present but inactive
67 (*Methanosphaera*) ¹⁶ or completely lost (*Thermoplasmata* methanogens) ⁶⁻⁷. Recent metagenomic
68 studies have uncovered three additional, deep lineages of potential methyl-reducing methanogens,
69 namely, Candidate class "*Methanofastidiosia*" within *Euryarchaeota* ²¹ and Candidate phyla

70 "Bathyarchaeota" and "Verstraetearchaeota"^{8,9}, supporting the earlier hypothesis that this is an
71 independently evolved, ancient pathway²².

72 The classical methylotrophic pathway of methanogenesis that has been characterized in
73 moderately halophilic members of *Methanosarcinales*²³, apparently dominates in hypersaline
74 conditions²³⁻²⁵. In contrast to the extremely halophilic haloarchaea, these microbes only tolerate
75 saturated salt conditions but optimally grow at moderate salinity (below 2-3 M Na⁺) using organic
76 compounds for osmotic balance ("salt-out" strategy)^{26,27}.

77 Our recent study of methanogenesis in hypersaline soda lakes identified methylotrophic
78 methanogenesis as the most active pathway. In addition, culture-independent analysis of the *mcrA*
79 gene, a unique marker of methanogens, identified a deep lineage that is only distantly related to other
80 methanogens²⁸. We observed no growth of these organisms upon addition of substrates for the
81 classical methanogenic pathways and concluded that they required distinct growth conditions. Here we
82 identify such conditions and describe the discovery and physiological, genomic and phylogenetic
83 features of a previously overlooked group of extremely halophilic, methyl-reducing methanogens.

84

85 **Discovery of an unknown deep lineage of extremely halophilic methanogens in hypersaline lakes**

86 *Sediment stimulation experiments*

87 Two deep-branching *mcrA* sequences have been previously detected in sediments from hypersaline
88 soda lakes in south-eastern Siberia²⁸. Attempts to stimulate the activity of these uncharacterized,
89 dormant methanogens by variation of conditions (temperature, pH and salinity) and substrates elicited
90 a positive response at extreme salinity (4 M Na⁺), pH (9.5-10), elevated temperature (above 48-55°C)
91 and in the presence of methylotrophic substrates together with formate or H₂ (the combination used in
92 the methyl-reducing pathway). The typical response involved a pronounced increase in methane
93 production upon combining methyl compounds with formate or H₂ (less active) compared to single
94 substrates (**Supplementary Figure 1 a**). The *mcrA* profiling of such incubations revealed two distinct
95 clusters closely related to the previously detected deep methanogenic lineage²⁸ (**Supplementary**
96 **Figure 2**).

97 The same approach was used with sediment slurries from hypersaline lakes with neutral pH
98 (with no previous evidence of the presence of methyl-reducing methanogens). In this case, enhanced
99 methane production under methyl-reducing conditions (MeOH/trimethylamine + formate) was also
100 observed at elevated temperatures (**Supplementary Figure 1 b,c**). The *mcrA* profiles indicated that
101 typical halophilic methylotrophic methanogens (*Methanohalophilus* and *Methanohalobium*) were
102 outcompeted at high temperature (50-60°C) by unknown, extremely halophilic methyl-reducers which
103 formed a sister clade to the sequences from methyl-reducing incubations of soda lakes sediments in
104 the *mcrA* tree (**Supplementary Figure 2**).

105

106 *Cultivation of the extremely halophilic methyl-reducing methanogens*

107 The active sediment incubations from hypersaline lakes (**Supplementary Table 1**) were used as an
108 enriched source to obtain the methyl-reducing methanogens in laboratory culture using synthetic
109 media with 2-4 M Na⁺, pH 7 (for salt lakes) or 9.5-10 (for soda lakes), supplemented with
110 MeOH/formate or trimethylamine (TMA)/formate and incubated at 48-60°C. Methane formation was
111 observed only at extreme salinity, close to saturation (4 M total Na⁺), but ceased after the original
112 sediment inoculum was diluted by 2-3 consecutive 1:100 transfers. Addition of colloidal FeSxH₂O
113 (soda lakes) or sterilized sediments (salt lakes), combined with filtration through 0.45 µm filters and
114 antibiotic treatment, yielded a pure culture from Siberian soda lakes (strain AMET1 [Alkaliphilic
115 Methylotrophic Thermophilic]), and 10 additional pure AMET cultures from hypersaline alkaline
116 lakes in various geographic locations. A similar approach resulted in three highly enriched cultures at
117 neutral pH from salt lakes (HMET [Halophilic Methylotrophic Thermophilic] cultures)
118 (**Supplementary Table 2**). Phylogenetic analysis of the marker genes showed that AMET and HMET
119 formed two potential genus-level groups that shared 90% 16S rRNA gene sequence identity.

120

121 **Microbiological characteristics of the methyl-reducing methanogens**

122

123 *Cell morphology and composition*

124 Both AMET and HMET possess small coccoid cells that are motile, in the case of AMET, and lack
125 F₄₂₀ autofluorescence that is typical of most methanogens. A thin, single-layer cell wall was present in

126 both groups (**Figure 1; Supplementary Figure 3**). At salt concentration below 1.5 M total Na⁺, the
127 cells lost integrity.

128 The extreme halophily of the discovered methanogens is unprecedented. The salt-tolerant
129 methylotrophs isolated so far from hypersaline habitats, such as *Methanohalobium*,
130 *Methanohalophilus* and *Methanosalsum*, all accumulate organic osmolytes ("salt-out"
131 osmoprotection). In contrast, no recognizable organic osmolytes were detected in AMET1 cells that,
132 instead, accumulated high intracellular concentrations of potassium [5.5 μmol/g protein or 2.2 M,
133 assuming the cell density of 1.2 mg/ml for haloarchaea²⁹ and the measured protein content of 30%].
134 This concentration is twofold lower than that normally observed inside the cells of haloarchaea (12- 13
135 μmol/g protein) but close to that of *Halanaerobium* (6.3 μmol/g protein), both of which have been
136 shown to employ the "salt-in" osmoprotection strategy^{30,31}. Furthermore, half of the sodium in the
137 medium is present in the form of carbonates, which possess exactly twofold less osmotic activity than
138 NaCl, resulting in decreased total osmotic pressure, and accordingly, a lower intracellular
139 concentration of osmolytes in extreme natronophiles³². This finding suggests that the extremely
140 halophilic methyl-reducing methanogens rely on potassium as the major osmolyte.

141 The AMET cell pellets were pinkish in color, suggestive of the presence of cytochromes
142 which was confirmed by difference spectra of a cell-free extract from AMET1 that showed peaks
143 characteristic of *b*-type cytochromes (**Supplementary Figure 4 a**). Given that the cytochrome-
144 containing methanogens of the order *Methanosarcinales* also synthesize the electron-transferring
145 quinone analogue methanophenazine³³, we attempted to detect this compound in AMET1. Indeed, two
146 yellow-colored autofluorescent hydrophobic fractions were recovered from the AMET1 cells, with
147 main masses of 562 and 580 Da, which behaved similar to methanophenazine from *Methanosarcina*
148 (mass 532 Da) upon chemical ionization (sequential cleavage of the 68 Da mass isoprene unit)
149 (**Supplementary Figure 4 b**).

150

151 *Growth physiology*

152 Both AMET and HMET are methyl-reducing heterotrophic methanogens utilizing C₁-methyl
153 compounds as *e*-acceptor, formate or H₂ as *e*-donor, and yeast extract or acetate as the C-source.

154 Growth of both groups of organisms was stimulated by addition of external CoM (up to 0.1 mM).
155 Despite the general metabolic similarity, the AMET cultures grew and survived long storage much
156 better than the HMET cultures. The AMET cultures grew best with MeOH as acceptor and formate as
157 donor (**Figure 2 a**). Apart from MeOH, slower growth was also observed with methylamines and
158 dimethylsulfide (**Figure 2 b**). In sharp contrast to the known methyl-reducing methanogens, H₂ was
159 less effective as the electron donor.

160 Both groups grew optimally around 50°C, with the upper limit at 60°C (**Figure 2 c**,
161 **Supplementary Figure 5**). The AMET isolates were obligate alkaliphiles, with optimum growth at
162 pH 9.5-9.8 (**Figure 2 d**), whereas the HMET cultures had an optimum at pH 6.8-7. The organisms of
163 both groups showed the fastest growth and the highest activity at salt-saturating conditions, and thus
164 qualified as extreme halo(natrono)philes (**Figure 2 e,f**).

165

166 *Effect of iron sulfides on growth and activity of AMET1*

167 Apart from hydrotroilite (FeS_xnH₂O), AMET1 also grew, albeit less actively, in the presence of
168 crystalline FeS, and yet less actively, with pyrite (FeS₂). No other forms of reduced iron minerals tested
169 (olivine, FeCO₃, magnetite, ferrotine (FeS_n) or various iron(II) silicates could replace FeS.
170 Furthermore, methanogenic activity of resting cells depleted for FeS showed dependence on FeS
171 addition (**Figure 3**). No methane was formed in the absence of either methyl acceptors or formate/H₂,
172 suggesting that Fe²⁺ likely served as a catalyst or regulator rather than a direct *e*-donor. The specific
173 cause(s) of the dependence of AMET growth on iron (II) sulfides remains to be identified.

174

175 *Comparative genomic analysis*

176 *General genome characteristics*

177 The general genome characteristics of AMET1 and HMET1 are given in **Table 1**. Based on
178 analysis of 218 core arCOGs³⁴, both genomes are nearly complete, with two genes missing from this
179 list in AMET1 and three in HMET1. Two of these genes are missing in both genomes (prefoldin
180 paralog GIM5 and deoxyhypusine synthase DYS1), suggesting that they were lost in the common
181 ancestor (**Supplementary Table 3**). The presence of tRNAs for all amino acids is another indication

182 of genome completeness. The high coverage of the AMET1 and HMET1 genomes by arCOGs implies
183 that the unique phenotype of these organisms is supported largely by the already well-sampled part of
184 the archaeal gene pool.

185

186 *Phylogenetic analysis and taxonomy*

187 A concatenated alignment of the 56 ribosomal proteins that are universally conserved in
188 complete archaeal genomes³⁵ including AMET1 and HMET1 was used for maximum likelihood tree
189 reconstruction (**Figure 4 a, Supplementary Table 3, Supplementary Data 1**). Both AMET1 and
190 HMET1 belong to a distinct clade, a sister taxon to the class *Halobacteria*, with 100% bootstrap
191 support (**Figure 4 a**). The 16S rRNA gene tree suggests that both organisms belong to the uncultured
192 SA1 group that was first identified in the brine-seawater interface of the Shaban Deep in the Red Sea³⁶
193 and subsequently in other hypersaline habitats³⁷ (**Supplementary Figure 6**). According to the rRNA
194 phylogeny, the group that includes AMET1 and HMET1 is well separated from the other classes in the
195 phylum Euryarchaeota, both methanogenic and non-methanogenic. The 16S rRNA sequences of
196 these organisms are equally distant from all classes in *Euryarchaeota* and fall within the range
197 of recently recommended values (80-86%) for the class level classification³⁸. Together, these
198 findings appear to justify classification of the SA1 group, including the AMET and HMET lineages, as
199 a separate euryarchaeal class "**Methanonatronarchaeia**". This class would be represented by two
200 distinct genera and species "**Methanonatronarchaeum thermophilum**" (AMET) and '**Candidatus**
201 **Methanohalarchaeum thermophilum**' (HMET).

202

203 *Comparative genomic analysis and reconstruction of main evolutionary events*

204 Using arCOG assignments and the results of previous phylogenomic analysis³⁹, we
205 reconstructed the major evolutionary events in the history of AMET1, HMET1 and *Halobacteria*
206 (**Figure 4 a and Supplementary Table 4**). This reconstruction indicates that evolution of the
207 HMET1-AMET1 lineage was dominated by gene loss, whereas *Halobacteria* acquired most of their
208 gene complement after the divergence from "Methanonatronarchaeia". As shown previously, the

209 common ancestor of *Methanomicrobia* and *Halobacteria* was a methanogen³⁹. The key genes coding
210 for components of the protein complexes involved in the classical methanogenesis pathways, such as
211 tetrahydromethanopterin S-methyltransferase (Mtr), F₄₂₀-reducing hydrogenase and Ftr, appear to have
212 been lost along the branch leading to the common ancestor of *Halobacteria* and
213 "Methanonatronarchaeia". After the divergence, *Halobacteria* continued to lose all other genes
214 involved in methanogenesis and acquire genes for aerobic and mostly heterotrophic pathways, whereas
215 "Methanonatronarchaeia" retained most pathways for anaerobic metabolism, while rewiring the
216 methanogenic pathways for the mixotrophic lifestyle (**Figure 5 a**). As in other cases, genome
217 reduction in "Methanonatronarchaeia" affected RNA modification, DNA repair and stress response
218 systems as well as surface protein structures³⁹. The subsequent gene loss occurred differentially in the
219 two groups of "Methanonatronarchaeia", suggesting adaptation to different ecological niches. The
220 HMET group lost chemotaxis and motility genes and shows signs of adaptation to heterotrophy,
221 whereas AMET retains the ability to synthesize most cellular building blocks at the expense of
222 transporter loss. The AMET strains are motile but lost attachment pili, which are present in the vast
223 majority of the species of the *Halobacteria-Methanomicrobia* clade⁴⁰, and many glycosyltransferases,
224 suggesting simplification of the surface protein structures. The presence of two complete CRISPR-Cas
225 systems in HMET1 compared to none in AMET1, along with the large excess of genes implicated in
226 anti-parasite defense and transposons in HMET1 (**Figure 5 c** and **Table 1**), further emphasize the
227 lifestyle differences indicating that HMET1 is subject to a much stronger pressure from mobile
228 elements than AMET1.

229

230 *Central metabolism reconstruction*

231 In agreement with the experimental results, genome analysis allowed us to identify the genes
232 of AMET1 and HMET1 that are implicated in energy flow and key reactions of biomass production,
233 which appear to be simple and straightforward (**Figure 6**). The main path starts with utilization of C₁
234 methyl-containing compounds for methane production by CoM methyltransferases and methyl-CoM
235 reductase complexes, respectively. Similar to the methyl-reducing *Methanomasillicoccales*⁶, the
236 genomes of AMET1 and, especially, HMET1 contains multiple operons encoding diverse

237 methyltransferases (**Supplementary Figure 7**). Methyl-reduction is coupled with ATP generation and
238 involves five membrane-associated complexes, namely, formate dehydrogenase, membrane-bound
239 heterodisulfide reductase HdrED, Ni,Fe hydrogenase I, multisubunit Na⁺/H⁺ antiporter and H⁺ -
240 transporting ATP synthase. The recently characterized complete biosynthetic pathway⁴¹ for coenzyme
241 F₄₃₀ is present in both genomes. In addition, membrane *b*-type cytochromes and methanophenazine-
242 like compounds are implicated in electron transport.

243 Pyruvate, the key entry point for biomass production, is generated through acetate
244 incorporation by acetyl-CoA synthetase (**Figure 6**). In a sharp contrast to most methanogens, both
245 genomes lack genes for tetrahydromethanopterin S-methyltransferase Mtr complex and
246 formylmethanofuran dehydrogenase Fwd complex, leaving all intermediate reactions, for which the
247 genes are present, unconnected to other pathways (**Figure 6**). All four recently reported deep lineages
248 of euryarchaeal methyl-reducing methanogens (*Methanomasillilicoccales* and '*Candidatus*
249 *Methanofastidiosa*') and those from the TACK superphylum ('*Candidatus* Bathyarchaeota' and
250 '*Candidatus* Verstraetearchaeota')^{8,9} lack the Mtr and Fwd complexes as well, but they also lack all
251 the genes involved in intermediate reactions. It is extremely unlikely that genes for all Mtr and Fwd
252 complex subunits are present in both AMET1 and HMET1 but were missed by sequencing. Thus,
253 these organisms might possess still unknown pathways to connect the intermediate reactions to the rest
254 of the metabolic network.

255 In addition to the main biosynthetic pathway, AMET1 and HMET1 possess genes for three
256 key reactions of anaplerotic CO₂ fixation, namely, malic enzyme, phosphoenolpyruvate carboxylase
257 and carbamoylphosphate synthase. Furthermore, complete gene sets for CO₂ fixation pathway through
258 archaeal RUBISCO are present in both genomes (**Figure 6**)⁴². The great majority of the genes
259 involved in the key biosynthetic pathways for amino acids, nucleotides, cofactors and lipids also were
260 identified in both genomes and found to be highly expressed in proteomic analysis, as revealed by
261 estimating the absolute protein amount based on the exponentially modified protein abundance index
262 (emPAI) (**Supplementary Table 6 and 7**). Interestingly, emPAI-based abundances follow an
263 exponential distribution in which 4 proteins involved in methanogenesis are among the 10 most highly
264 expressed proteins.

265 HMET1 seems to be more metabolically versatile compared with AMET1, especially with
266 respect to methanogenesis as well as amino acid and sugar metabolism (**Figure 5 b** and **5 c**). However,
267 unlike AMET1, HMET1 lacks several genes for cofactor biosynthesis, such as quinolinate synthase
268 NadA and nicotinate-nucleotide pyrophosphorylase NadC, both involved in NAD biosynthesis;
269 uroporphyrinogen-III decarboxylase HemE and protoporphyrinogen IX oxidase HemG involved in
270 heme biosynthesis, sulfopyruvate decarboxylase involved in CoM biosynthesis and *cofCED* genes for
271 the coenzyme F₄₂₀ biosynthesis enzyme complex. This shortage of biosynthetic enzymes is consistent
272 with experimental observations on poorer growth and survival of HMET in culture compared to
273 AMET.

274

275 *Adaptation to extreme salinity*

276 Given that acidification of proteins is a common feature of the "salt-in" osmotic strategy, we estimated
277 isoelectric points for the proteomes of a large representative set of halophilic and non-halophilic
278 archaea and bacteria, and compared the distributions as described under Materials and Methods
279 (**Supplementary Table 5**). The distributions of isoelectric points in the AMET1 and HMET1
280 proteomes are similar to those of moderately halophilic archaea and bacteria, with the notable
281 exception of their closest relatives, the extremely halophilic *Halobacteria*, which form a distinct cloud
282 of extremely acidic proteomes (**Figure 5 d**). This separation indicates that the proteome acidity of
283 *Halobacteria* dramatically changed after the divergence from "Methanonatronarchaeia" that appear to
284 be an evolutionary intermediate on the path from methanogens to extreme halophiles. In agreement
285 with the "salt-in" osmoprotection strategy, AMET1 and HMET1 encode a variety of K⁺ transporters
286 (arCOG01960) but show no enrichment of transporters for known organic osmolytes, such as glycine,
287 betaine, ectoine, or glycerol, compared with other archaea (**Supplementary Table 3**). On more
288 general grounds, the "salt-out" strategy appears unlikely and perhaps unfeasible for extremely
289 halophilic secondary anaerobes with relatively low energy yield. Taken together, these considerations
290 suggest that the adaptation of "Methanonatronarchaeia" to the extreme salinity relies on the "salt-in"
291 strategy. Whether these organisms possess additional mechanisms for cation-binding to compensate

292 for the relatively low proteome acidity, remains to be determined, but it is also possible that the main
293 counter-anion, in this case, is Cl⁻.

294 Analysis of the AMET1 and HMET1 protein complements revealed a major expansion of the
295 UspA family of stress response proteins with likely chaperonin function that could contribute to the
296 structural stability of intracellular proteins (**Supplementary Figure 8**). Finally, we identified several
297 arCOGs consisting of uncharacterized membrane proteins (eg. arCOG04755, arCOG04622,
298 arCOG04619) that are specifically shared by AMET1, HMET1 and the majority of *Halobacteria*
299 (**Supplementary Table 3**). Some of these proteins contain pleckstrin homology domains, which
300 contribute to the mechanical stability of membranes in eukaryotes⁴³ and might play a similar role in
301 "Methanonatronarchaeia".

302 Notably, AMET1 protein expression analysis showed that the DNA/RNA-binding protein
303 Alba, an archaeal histone and one of the UspA family proteins were among the ten most abundant
304 proteins (**Supplementary Table 6**). These proteins contribute to RNA, DNA and protein stability and
305 might play important roles in supporting growth under extreme salinity conditions.

306

307 *Implications for the origin of methanogenesis*

308 In previous phylogenetic analyses of the methyl coenzyme M reductase complex (McrABCD)
309 subunits, the topology of the tree for these proteins generally reproduced the ribosomal protein-based
310 phylogeny^{13,22}. In the present phylogenetic analysis that used different protein sets and methods,
311 AMET1/HMET1, *Methanomasilliicoccales*¹³, ANME1 group⁴⁴ and '*Candidatus* Methanofastidiosa'
312 (WSA2 group)²¹ clustered together with high confidence (**Supplementary Figure 9 and 10,**
313 **Supplementary Data 2, 3 and 4**). This topology differs from the topology of the ribosomal protein
314 tree (**Figure 4 a**). This discrepancy could result from a combination of multiple horizontal transfers of
315 *mcrABCD* genes, differential gain and loss of paralogs, insufficient sampling of rare lineages, and
316 phylogenetic artefacts caused by variation of evolutionary rates. Indeed, we observed a complex
317 evolutionary history of McrA, including many lineage-specific duplications and losses
318 (**Supplementary Figure 9**).

319 Reconstruction of evolutionary events and mapping the methanogens onto the archaeal tree
320 suggests that the origin of methanogenesis dates back to the common ancestor of archaea, with
321 multiple, independent losses in various clades (**Figure 5 a**). The loss of the methanogenic pathways
322 often proceeds through intermediate stages as clearly observed both in "Methanonatronarchaeia" and
323 *Methanomasilliicoccales* (**Figure 5 a**). Comparison of the gene sets (arCOGs) enriched in different
324 groups of methanogens (**Supplementary Table 3**) using multidimensional scaling revealed distinct
325 patterns of gene loss in "Methanonatronarchaeia", *Methanomasilliicoccales*, ANME1 and '*Candidatus*
326 *Bathyarchaeota*', in agreement with the independent gene loss scenario (**Figure 5 e**). Notwithstanding
327 these arguments, the possibility that '*Candidatus Bathyarchaeota*' and ANME1 acquired
328 methanogenesis via HGT cannot be ruled out, relegating its origin to the common ancestor of
329 *Euryarchaeota*. Further sampling of diverse archaeal genomes should resolve this issue.

330

331 **Conclusions**

332 We discovered an unknown, deep euryarchaeal lineage of moderately thermophilic and extremely
333 halo(natrono)philic methanogens that thrive in hypersaline lakes. This group is not monophyletic with
334 the other methanogens but forms a separate, class-level lineage "Methanonatronarchaeia" that is most
335 closely related to *Halobacteria*. The "Methanonatronarchaeia" possess the methyl-reducing type of
336 methanogenesis, where C₁-methylated compounds serve as acceptor and formate or H₂ are external
337 electron donor, but differ from all other methanogens with this type of metabolism in the electron
338 transport mechanism. In contrast to all previously described halophilic methanogens,
339 "Methanonatronarchaeia" grow optimally in saturated salt brines and probably employ potassium-
340 based osmoprotection, similar to extremely halophilic archaea and *Halanaerobiales*. This discovery is
341 expected to have substantial impact on our understanding of biogeochemistry, ecology and evolution
342 of the globally important microbial methanogenesis.

343

344 **Methods**

345

346 *Samples*

347 Anaerobic sediments (depth from 5 to 15 cm) and near bottom brines were obtained in hypersaline soda and salt
348 lakes in south-western Siberia (Altai region) and south Russia Volgograd region and Crimea) in July of 2013-

349 2015. The salt concentration varied from 100 to 400 g/l and the pH from 6.5-8 (salt lakes) to 9.8-10.5 (soda
350 lakes). In addition, sediments from Wadi al Natrun alkaline hypersaline lakes in Egypt (October 2000) and
351 alkaline hypersaline Searles Lake in California (April 2005) were used as inoculum in methanogenic enrichment
352 cultures. The details of the lake properties are given in **Supplementary Table 1**. The methanogenic potential
353 activity measurements followed by the *mcrA* analysis have been performed in 1:1 sediment-brine slurries as
354 described previously²⁸.

356 *Enrichment and cultivation conditions*

357 For soda lakes, the sodium carbonate-based mineral media containing 1-4 M total Na⁺ strongly buffered at pH 10
358^{28,45} was used for enrichments. For salt lakes, the mineral medium containing 4 M NaCl and 0.1 M KCl buffered
359 with 50 mM K phosphates at pH 6.8 was employed. Both media after sterilization were supplied with 1 ml/l of
360 acidic⁴⁶ and alkaline W/Se⁴⁷ trace metal solutions, 1 ml/l of vitamin mix⁴⁶, 4 mM NH₄Cl, 20 mg/l yeast extract
361 and 0.1 mM filter-sterilized CoM. The media were dispensed in serum bottles with butyl rubber stoppers of
362 various capacity at 50 (H₂) - 80% (formate) filled volumes, made anoxic with 5 cycles of argon flushing-
363 evacuation and finally reduced by the addition of 1 mM Na₂S and 1 drop/100 ml of 10% dithionite in 1 M
364 NaHCO₃. H₂ was added on the top of argon atmosphere at 0.5 bar overpressure, formate and methanol - at 50
365 mM, methylamines - at 10 mM, methyl- and dimethyl sulfides - at 5 mM. In case of methylamines, ammonium
366 was omitted from the basic medium. The incubation temperature varied from 30 to 65°C. Analyses of growth
367 parameters, pH-salt profiling of growth and activity of washed cells, optical and electron microscopy and
368 chemical analyses were performed as described previously^{28,45}.

369

370 *Biomass composition*

371 The presence of organic compatible solutes was tested by using HPLC and ¹H-NMR after extraction from dry
372 cells with EtOH and the intracellular potassium concentration was quantified by ICP-MS. The presence of the
373 methanophenazine analogues was analyzed in acetone extract from lyophilized cells, followed by TLC separation,
374 reextraction with MeOH-chloroform mixture and MS-MS spectrometry.

375

376 *Genome sequencing and assembly*

377 The genomic DNA from pure and highly enriched cultures was obtained by using UltraClean Microbial
378 DNA Extraction Kit (MoBio Laboratories). The genome sequencing, assembly and automatic annotation of a
379 pure culture from soda lakes and of a metagenome from a highly enriched salt lake culture was performed by
380 BaseClear (Leiden, The Netherlands) using a combination of Illumina and PacBio platforms. Kmer
381 tetranucleotide frequency analysis was used to identify contigs that are likely belong to HMET1 (meta)genome.
382 Genome completeness has been estimated as described previously⁴⁸.

383

384 *Genome annotation and sequence analysis*

385 The final gene call has been combined from results by PROKKA⁴⁹ and GeneMarkS⁵⁰ pipelines. All
386 protein coding genes were assigned to most recent archaeal Clusters of Orthologous Groups, arCOGs as
387 described previously³⁴. Protein annotations were obtained by a combination of arCOGs and PROKKA
388 annotations and, in case of conflict, the respective protein have been manually reanalyzed using PSI-BLAST⁵¹
389 and HHpred results⁵² and their annotations were modified if necessary. The final assembled and annotated
390 genomic datasets were deposited in GenBank under accession numbers: MRZU00000000 and
391 MSDW00000000.

392 Other genomes related to the comparison described here were taken from GenBank (March 2016) and if
393 it was necessary ORFs have been predicted using GeneMarkS⁵⁰.

394 Protein sequences were aligned using MUSCLE⁵³. Alignments for the tree reconstruction have been
395 filtered to obtain informative position as described previously³⁴. Approximate maximum likelihood
396 phylogenetic trees were reconstructed using FastTree⁵⁴ and PHYML⁵⁵ methods. The PHYML program was
397 used for the phylogenetic tree reconstruction from an alignment of 51 concatenated ribosomal proteins (287
398 species, 8072 positions), with the following parameters: LG matrix, gamma distributed site rates, default
399 frequencies which were determined by PROTTEST program⁵⁶. Support values were estimated using an
400 approximate Bayesian method implemented in PhyML. For McrA, multiple alignment (145 sequences and 553
401 positions) was used for tree reconstruction using PhyML and PROTTEST as described above.

402 Two sets of genes reconstructed previously using the program COUNT³⁹, which employs a Markov
403 chain gene birth and death model, for the ancestors of *Halobacteriales* *Halobacteriales*/*Methanomicrobiales*
404 were used to infer gene gains and losses on the branches leading to *Halobacteriales*, and the discovered clade of
405 extremely halophilic methanogens. We considered an arCOG to be present in these two clades when the
406 respective COUNT probability was higher than 50%. Further reconstruction was done using a straightforward
407 parsimony approach as explained in detail in **Supplementary Table 4**.

408 Isoelectric points (pI) of individual proteins were calculated according to Bjellqvist et al.⁵⁷ using the pK
409 values from the EMBOSS suite⁵⁸. Genome-wide distributions of the protein pI were obtained as the probability
410 density estimates at 100 points in the 2.0 – 14.0 pH range using the Gaussian kernel method⁵⁹. Kullback-Leibler
411 divergence of the pI distributions for the pair of genomes *A* and *B*, $D_{KL}(A|B)$ was computed for all ordered pairs
412 of the set. The distance between the genomes was estimated as $D(A,B) = D(B,A) = (D_{KL}(A|B) + D_{KL}(B|A))/2$ ⁶⁰.
413 The matrix of genome distances was projected into a two-dimensional space using the Classical
414 Multidimensional Scaling method^{61,62} as implemented in the R package⁶³.

416 *Proteomics*

417 Proteomic analyses were conducted using the soda lake pure culture AMET1 (48°C, MeOH+formate)
418 and the salt lake enrichment HMET1 (37°C, TMA+H₂) (**Supplementary Table 6 and 7**). Cell pellets were
419 dissolved in lysis buffer (8 M urea, 2 M thiourea, 5% CHAPS, 5 mM TCEP-HCl and a protease inhibitors
420 cocktail). Homogenization of the cells was achieved by ultra-sonication for 5 min on ultrasonic bath. After
421 homogenization, the lysed cells were centrifuged at 20,000×g for 10 min at 4 °C, and the supernatant containing
422 the solubilized proteins was used for LC-MS/MS experiment. All samples were precipitated by
423 methanol/chloroform method and re-suspended in a multi-chaotropic sample solution (7 M urea, 2 M thiourea,
424 100 mM TEAB; pH 7.5). Total protein concentration was determined using Pierce 660 nm protein assay
425 (Thermo). 40 µg of protein from each sample were reduced with 2 µL of 50mM Tris(2-carboxyethyl) phosphine
426 (TCEP, SCIEX), pH 8.0, at 37°C for 60 min and followed by 1 µL of 200mM cysteine-blocking reagent (methyl
427 methanethiosulfonate (MMTS, Pierce) for 10 min at room temperature. Samples were diluted up to 140 µL to
428 reduce urea concentration with 25mM TEAB. Digestions were initiated by adding 2 µg Pierce MS-grade trypsin
429 (Thermo Scientific) to each sample in a ratio 1:20 (w/w), which were then incubated at 37°C overnight on a
430 shaker. Sample digestions were evaporated to dryness in a vacuum concentrator and then desalted onto StageTip
431 C18 Pipette tips (Thermo Scientific) until the mass spectrometric analysis.

432 A 1 µg aliquot of each sample was subjected to 1D-nano LC ESI-MSMS analysis using a nano liquid
433 chromatography system (Eksigent Technologies nanoLC Ultra 1D plus, AB SCIEX, Foster City, CA) coupled to
434 high speed Triple TOF 5600 mass spectrometer (SCIEX, Foster City, CA) with a Nanospray III source. The
435 analytical column used was a silica-based reversed phase Acquity UPLC M-Class Peptide BEH C18 Column, 75
436 µm × 150 mm, 1.7 µm particle size and 130 Å pore size (Waters). The trap column was a C18 Acclaim
437 PepMapTM 100 (Thermo Scientific), 100 µm × 2 cm, 5 µm particle diameter, 100 Å pore size, switched on-line
438 with the analytical column. The loading pump delivered a solution of 0.1% formic acid in water at 2 µl/min. The
439 nano-pump provided a flow-rate of 250 nl/min and was operated under gradient elution conditions. Peptides
440 were separated using a 250 minutes gradient ranging from 2% to 90% mobile phase B (mobile phase A: 2%
441 acetonitrile, 0.1% formic acid; mobile phase B: 100% acetonitrile, 0.1% formic acid). Injection volume was 5 µl.

442 Data acquisition was performed with a TripleTOF 5600 System (SCIEX, Foster City, CA). Data was
443 acquired using an ionspray voltage floating (ISVF) 2300 V, curtain gas (CUR) 35, interface heater temperature
444 (IHT) 150, ion source gas 1 (GS1) 25, declustering potential (DP) 100 V. All data was acquired using
445 information-dependent acquisition (IDA) mode with Analyst TF 1.7 software (SCIEX, Foster City, CA). For
446 IDA parameters, 0.25s MS survey scan in the mass range of 350–1250 Da were followed by 35 MS/MS scans of
447 100ms in the mass range of 100–1800 (total cycle time: 4 s). Switching criteria were set to ions greater than mass
448 to charge ratio (m/z) 350 and smaller than m/z 1250 with charge state of 2–5 and an abundance threshold of
449 more than 90 counts (cps). Former target ions were excluded for 15s. IDA rolling collision energy (CE)
450 parameters script was used for automatically controlling the CE.

451 MS and MS/MS data obtained for individual samples were processed using Analyst® TF 1.7 Software
452 (SCIEX). The reconstituted AMET1 and HMET1 chromosome sequence was used to generate the database for
453 protein identification using the Mascot Server v. 2.5.1 (Matrix Science, London, UK). Search parameters were
454 set as follows: carbamidomethyl (C) as fixed modification and acetyl (Protein N-term), Gln to pyro-Glu (N-term
455 Q), Glu to pyro-Glu (N-term E) and methionine oxidation as variable modifications. Peptide mass tolerance was
456 set to 25 ppm and 0.05 Da for fragment masses, also 2 missed cleavages were allowed. The confidence interval
457 for protein identification was set to ≥ 95% (p<0.05) and only peptides with an individual ion score above the 1%
458 False Discovery Rates (FDR) at PSM level were considered correctly identified. False Discovery Rates were
459 manually calculated. The threshold of only one identified peptide per protein identification was used because

460 FDR controlled experiments counter intuitively suffer from the two-peptide rule⁶⁴. To rank the protein

461 abundance in each sample, the Exponentially Modified Protein Abundance Index (emPAI) was used in the
462 present study as a relative quantitation score of the proteins in a complex mixture based on protein coverage by
463 the peptide matches in a database search result⁶². Although the emPAI is not as accurate as quantification using
464 synthesized peptide standards, it is quite useful for obtaining a broad overview of proteome profiles.

465

466 **Acknowledgements.** DYS was supported by STW (project 12226), Gravitation-SIAM Program (grant
467 24002002, Dutch Ministry of Education and Science) and by RFBR (grant 16-04-00035). KSM, YIW and EVK
468 are supported by the intramural program of the U.S. Department of Health and Human Services (to the National
469 Library of Medicine). The proteomic analysis was performed in the Proteomics Facility of The Spanish National
470 Center for Biotechnology (CNB-CSIC) that belongs to ProteoRed, PRB2-ISCI, supported by grant PT13/0001.
471 This project has received funding from the European Union's Horizon 2020 research and innovation program
472 [Blue Growth: Unlocking the potential of Seas and Oceans] under grant agreement No [634486]. This work was
473 further funded by grant BIO2014-54494-R from the Spanish Ministry of Economy, Industry and
474 Competitiveness.

475
476 **Author contributions.** D.Y.S. performed the field work, the sediment activity incubations, enrichment and
477 isolation of pure cultures and microbiological investigation of enriched and pure cultures. B.A. and A.Y.M.
478 analyzed the *mcrA* and 16S rRNA genes in sediments and methanogenic cultures. M.F., P.N.G., S.C. and M.C.M.
479 were responsible for the proteomic analysis. E.G. analyzed compatible solutes. K.S.M., Y.I.W. and E.V.K.
480 performed genomic analysis and evolutionary reconstructions. D.Y.S., K.S.M. and E.V.K. wrote the paper.
481 M.C.M.L. oversaw the project and participated in the data interpretation and discussion.

482
483 **Competing interests.** The authors declare no competing financial interests.

484 **References**

- 485 1 Ferry, J. G. & Kastead, K. A. in *Archaea: Molecular and Cellular Biology* (ed R.
486 Cavicchioli) 288-214 (ASM Press, 2007).
- 487 2 Conrad, R. The global methane cycle: recent advances in understanding the microbial
488 processes involved. *Environmental microbiology reports* **1**, 285-292,
489 doi:10.1111/j.1758-2229.2009.00038.x (2009).
- 490 3 Agency, U. S. E. P. (ed US-EPA) (2016).
- 491 4 Garrity, G. M. & Holt, J. G. in *Bergey's Manual of Systematics of Archaea and*
492 *Bacteria* Vol. 1 (John Wiley & Sons, Inc. , 2015).
- 493 5 Iino, T. *et al.* Candidatus Methanogram caenicola: a novel methanogen from the
494 anaerobic digested sludge, and proposal of Methanomassiliicoccales fam. nov. and
495 Methanomassiliicoccales ord. nov., for a methanogenic lineage of the class
496 Thermoplasmata. *Microbes and environments* **28**, 244-250 (2013).
- 497 6 Borrel, G. *et al.* Comparative genomics highlights the unique biology of
498 Methanomassiliicoccales, a Thermoplasmatales-related seventh order of methanogenic
499 archaea that encodes pyrrolysine. *BMC genomics* **15**, 679, doi:10.1186/1471-2164-15-
500 679 (2014).
- 501 7 Lang, K. *et al.* New mode of energy metabolism in the seventh order of methanogens
502 as revealed by comparative genome analysis of "Candidatus methanoplasma
503 termitum". *Applied and environmental microbiology* **81**, 1338-1352,
504 doi:10.1128/AEM.03389-14 (2015).
- 505 8 Evans, P. N. *et al.* Methane metabolism in the archaeal phylum Bathyarchaeota
506 revealed by genome-centric metagenomics. *Science* **350**, 434-438,
507 doi:10.1126/science.aac7745 (2015).
- 508 9 Vanwonterghem, I. *et al.* Methylophilic methanogenesis discovered in the archaeal
509 phylum Verstraetearchaeota. *Nature microbiology* **1**, 16170,
510 doi:10.1038/nmicrobiol.2016.170 (2016).
- 511 10 Hedderich, R. & Whitman, W. B. in *The Prokaryotes – Prokaryotic Physiology and*
512 *Biochemistry* (ed E. Rosenberg) 636-663 (Springer-Verlag, 2013).
- 513 11 Liu, Y. & Whitman, W. B. Metabolic, phylogenetic, and ecological diversity of the
514 methanogenic archaea. *Annals of the New York Academy of Sciences* **1125**, 171-189,
515 doi:10.1196/annals.1419.019 (2008).
- 516 12 Thauer, R. K., Kaster, A. K., Seedorf, H., Buckel, W. & Hedderich, R. Methanogenic
517 archaea: ecologically relevant differences in energy conservation. *Nature reviews.*
518 *Microbiology* **6**, 579-591, doi:10.1038/nrmicro1931 (2008).
- 519 13 Borrel, G. *et al.* Phylogenomic data support a seventh order of Methylophilic
520 methanogens and provide insights into the evolution of Methanogenesis. *Genome*
521 *biology and evolution* **5**, 1769-1780, doi:10.1093/gbe/evt128 (2013).
- 522 14 Dridi, B., Fardeau, M. L., Ollivier, B., Raoult, D. & Drancourt, M.
523 Methanomassiliicoccus luminyensis gen. nov., sp. nov., a methanogenic archaeon
524 isolated from human faeces. *International journal of systematic and evolutionary*
525 *microbiology* **62**, 1902-1907, doi:10.1099/ijs.0.033712-0 (2012).
- 526 15 Paul, K., Nonoh, J. O., Mikulski, L. & Brune, A. "Methanoplasmatales,"
527 Thermoplasmatales-related archaea in termite guts and other environments, are the
528 seventh order of methanogens. *Applied and environmental microbiology* **78**, 8245-
529 8253, doi:10.1128/AEM.02193-12 (2012).
- 530 16 Fricke, W. F. *et al.* The genome sequence of Methanosphaera stadtmanae reveals why
531 this human intestinal archaeon is restricted to methanol and H₂ for methane formation

- 532 and ATP synthesis. *Journal of bacteriology* **188**, 642-658, doi:10.1128/JB.188.2.642-
533 658.2006 (2006).
- 534 17 Miller, T. L. & Wolin, M. J. *Methanosphaera stadtmaniae* gen. nov., sp. nov.: a
535 species that forms methane by reducing methanol with hydrogen. *Archives of*
536 *microbiology* **141**, 116-122 (1985).
- 537 18 Sprenger, W. W., Hackstein, J. H. & Keltjens, J. T. The energy metabolism of
538 *Methanomicrococcus blatticola*: physiological and biochemical aspects. *Antonie van*
539 *Leeuwenhoek* **87**, 289-299, doi:10.1007/s10482-004-5941-5 (2005).
- 540 19 Sprenger, W. W., Hackstein, J. H. & Keltjens, J. T. The competitive success of
541 *Methanomicrococcus blatticola*, a dominant methylotrophic methanogen in the
542 cockroach hindgut, is supported by high substrate affinities and favorable
543 thermodynamics. *FEMS microbiology ecology* **60**, 266-275, doi:10.1111/j.1574-
544 6941.2007.00287.x (2007).
- 545 20 Sprenger, W. W., van Belzen, M. C., Rosenberg, J., Hackstein, J. H. & Keltjens, J. T.
546 *Methanomicrococcus blatticola* gen. nov., sp. nov., a methanol- and methylamine-
547 reducing methanogen from the hindgut of the cockroach *Periplaneta americana*.
548 *International journal of systematic and evolutionary microbiology* **50 Pt 6**, 1989-
549 1999, doi:10.1099/00207713-50-6-1989 (2000).
- 550 21 Nobu, M. K., Narihiro, T., Kuroda, K., Mei, R. & Liu, W. T. Chasing the elusive
551 Euryarchaeota class WSA2: genomes reveal a uniquely fastidious methyl-reducing
552 methanogen. *The ISME journal* **10**, 2478-2487, doi:10.1038/ismej.2016.33 (2016).
- 553 22 Borrel, G., Adam, P. S. & Gribaldo, S. Methanogenesis and the Wood-Ljungdahl
554 Pathway: An Ancient, Versatile, and Fragile Association. *Genome biology and*
555 *evolution* **8**, 1706-1711, doi:10.1093/gbe/evw114 (2016).
- 556 23 McGenity, T. J. in *Handbook of Hydrocarbon and Lipid Microbiology* (ed K.N.
557 Timmis) 665-679 (Springer-Verlag, 2010).
- 558 24 Kelley, C. A., Poole, J. A., Tazaz, A. M., Chanton, J. P. & Bebout, B. M. Substrate
559 limitation for methanogenesis in hypersaline environments. *Astrobiology* **12**, 89-97,
560 doi:10.1089/ast.2011.0703 (2012).
- 561 25 Oremland, R. S. & King, G. M. in *Microbial mats. Physiological ecology of benthic*
562 *microbial communities* (eds Y. Cohen & E. Rosenberg) 180-190 (American Society
563 for Microbiology, 1989).
- 564 26 Martin, D. D., Ciulla, R. A. & Roberts, M. F. Osmoadaptation in archaea. *Applied and*
565 *environmental microbiology* **65**, 1815-1825 (1999).
- 566 27 Menaia, J. A. G. F. Osmotics of halophilic methanogenic archaeobacteria. *Scholar*
567 *Archive paper* (1992).
- 568 28 Sorokin, D. Y. *et al.* Methanogenesis at extremely haloalkaline conditions in the soda
569 lakes of Kulunda Steppe (Altai, Russia). *FEMS microbiology ecology* **91**,
570 doi:10.1093/femsec/fiv016 (2015).
- 571 29 Ginzburg, M., Sachs, L. & Ginzburg, B. Z. Ion metabolism in a Halobacterium. I.
572 Influence of age of culture on intracellular concentrations. *The Journal of general*
573 *physiology* **55**, 187-207 (1970).
- 574 30 Elevi Bardavid, R. & Oren, A. The amino acid composition of proteins from anaerobic
575 halophilic bacteria of the order Halanaerobiales. *Extremophiles : life under extreme*
576 *conditions* **16**, 567-572, doi:10.1007/s00792-012-0455-y (2012).
- 577 31 Oren, A. Life at high salt concentrations, intracellular KCl concentrations, and acidic
578 proteomes. *Frontiers in microbiology* **4**, 315, doi:10.3389/fmicb.2013.00315 (2013).
- 579 32 Sorokin, D. Y., Banciu, H. L. & Muyzer, G. Functional microbiology of soda lakes.
580 *Current opinion in microbiology* **25**, 88-96, doi:10.1016/j.mib.2015.05.004 (2015).

- 581 33 Abken, H. J. *et al.* Isolation and characterization of methanophenazine and function of
582 phenazines in membrane-bound electron transport of *Methanosarcina mazei* Go1.
583 *Journal of bacteriology* **180**, 2027-2032 (1998).
- 584 34 Makarova, K. S., Wolf, Y. I. & Koonin, E. V. Archaeal Clusters of Orthologous Genes
585 (arCOGs): An Update and Application for Analysis of Shared Features between
586 Thermococcales, Methanococcales, and Methanobacteriales. *Life (Basel)* **5**, 818-840,
587 doi:life5010818 [pii] 10.3390/life5010818 (2015).
- 588 35 Yutin, N., Puigbo, P., Koonin, E. V. & Wolf, Y. I. Phylogenomics of prokaryotic
589 ribosomal proteins. *PLoS One* **7**, e36972, doi:10.1371/journal.pone.0036972 PONE-
590 D-11-23203 [pii] (2012).
- 591 36 Eder, W., Schmidt, M., Koch, M., Garbe-Schonberg, D. & Huber, R. Prokaryotic
592 phylogenetic diversity and corresponding geochemical data of the brine-seawater
593 interface of the Shaban Deep, Red Sea. *Environmental microbiology* **4**, 758-763
594 (2002).
- 595 37 Jiang, H. *et al.* Microbial response to salinity change in Lake Chaka, a hypersaline
596 lake on Tibetan plateau. *Environmental microbiology* **9**, 2603-2621,
597 doi:10.1111/j.1462-2920.2007.01377.x (2007).
- 598 38 Yarza, P. *et al.* Uniting the classification of cultured and uncultured bacteria and
599 archaea using 16S rRNA gene sequences. *Nature reviews. Microbiology* **12**, 635-645,
600 doi:10.1038/nrmicro3330 (2014).
- 601 39 Wolf, Y. I., Makarova, K. S., Yutin, N. & Koonin, E. V. Updated clusters of
602 orthologous genes for Archaea: a complex ancestor of the Archaea and the byways of
603 horizontal gene transfer. *Biol Direct* **7**, 46, doi:10.1186/1745-6150-7-46 1745-6150-7-
604 46 [pii] (2012).
- 605 40 Makarova, K. S., Koonin, E. V. & Albers, S. V. Diversity and Evolution of Type IV
606 pili Systems in Archaea. *Frontiers in microbiology* **7**, 667,
607 doi:10.3389/fmicb.2016.00667 (2016).
- 608 41 Zheng, K., Ngo, P. D., Owens, V. L., Yang, X. P. & Mansoorabadi, S. O. The
609 biosynthetic pathway of coenzyme F430 in methanogenic and methanotrophic
610 archaea. *Science* **354**, 339-342, doi:10.1126/science.aag2947 (2016).
- 611 42 Aono, R. *et al.* Enzymatic characterization of AMP phosphorylase and ribose-1,5-
612 bisphosphate isomerase functioning in an archaeal AMP metabolic pathway. *Journal*
613 *of bacteriology* **194**, 6847-6855, doi:10.1128/JB.01335-12 (2012).
- 614 43 Baines, A. J. Evolution of spectrin function in cytoskeletal and membrane networks.
615 *Biochemical Society transactions* **37**, 796-803, doi:10.1042/BST0370796 (2009).
- 616 44 Hallam, S. J., Girguis, P. R., Preston, C. M., Richardson, P. M. & DeLong, E. F.
617 Identification of methyl coenzyme M reductase A (*mcrA*) genes associated with
618 methane-oxidizing archaea. *Applied and environmental microbiology* **69**, 5483-5491
619 (2003).
- 620 45 Sorokin, D. Y. *et al.* *Methanosalsum natronophilum* sp. nov., and *Methanocalculus*
621 *alkaliphilus* sp. nov., haloalkaliphilic methanogens from hypersaline soda lakes.
622 *International journal of systematic and evolutionary microbiology* **65**, 3739-3745,
623 doi:10.1099/ijsem.0.000488 (2015).
- 624 46 Pfennig, N. & Lippert, K. D. Über das Vitamin B12-Bedürfnis phototropher
625 Schwefelbakterien. *Arch. Mikrobiol.* **55**, 245-256 (1966).
- 626 47 Plugge, C. M. Anoxic media design, preparation, and considerations. *Methods in*
627 *enzymology* **397**, 3-16, doi:10.1016/S0076-6879(05)97001-8 (2005).
- 628 48 Podar, M. *et al.* Insights into archaeal evolution and symbiosis from the genomes of a
629 nanoarchaeon and its inferred crenarchaeal host from Obsidian Pool, Yellowstone
630 National Park. *Biology direct* **8**, 9, doi:10.1186/1745-6150-8-9 (2013).

631 49 Seemann, T. Prokka: rapid prokaryotic genome annotation. *Bioinformatics* **30**, 2068-
632 2069, doi:10.1093/bioinformatics/btu153 (2014).

633 50 Besemer, J., Lomsadze, A. & Borodovsky, M. GeneMarkS: a self-training method for
634 prediction of gene starts in microbial genomes. Implications for finding sequence
635 motifs in regulatory regions. *Nucleic Acids Res* **29**, 2607-2618 (2001).

636 51 Altschul, S. F. *et al.* Gapped BLAST and PSI-BLAST: a new generation of protein
637 database search programs. *Nucleic Acids Res* **25**, 3389-3402 (1997).

638 52 Soding, J., Biegert, A. & Lupas, A. N. The HHpred interactive server for protein
639 homology detection and structure prediction. *Nucleic Acids Res* **33**, W244-248,
640 doi:10.1093/nar/gki408 (2005).

641 53 Edgar, R. C. MUSCLE: multiple sequence alignment with high accuracy and high
642 throughput. *Nucleic Acids Res* **32**, 1792-1797 (2004).

643 54 Price, M. N., Dehal, P. S. & Arkin, A. P. FastTree 2--approximately maximum-
644 likelihood trees for large alignments. *PLoS One* **5**, e9490,
645 doi:10.1371/journal.pone.0009490 (2010).

646 55 Guindon, S. *et al.* New algorithms and methods to estimate maximum-likelihood
647 phylogenies: assessing the performance of PhyML 3.0. *Systematic biology* **59**, 307-
648 321, doi:10.1093/sysbio/syq010 (2010).

649 56 Darriba, D., Taboada, G. L., Doallo, R. & Posada, D. ProtTest 3: fast selection of best-
650 fit models of protein evolution. *Bioinformatics* **27**, 1164-1165,
651 doi:10.1093/bioinformatics/btr088 (2011).

652 57 Bjellqvist, B. *et al.* The focusing positions of polypeptides in immobilized pH
653 gradients can be predicted from their amino acid sequences. *Electrophoresis* **14**, 1023-
654 1031 (1993).

655 58 Rice, P., Longden, I. & Bleasby, A. EMBOSS: the European Molecular Biology Open
656 Software Suite. *Trends in genetics : TIG* **16**, 276-277 (2000).

657 59 Parzen, E. On Estimation of a Probability Density Function and Mode. *Ann. Math. Statist.* **33**, 1065-1076 (1962).

658 60 Kullback, S. & Leibler, R. A. On information and sufficiency. *Ann. Math. Stat.* **22**, 79-
659 86 (1951).

660 61 Gower, J. C. Some distance properties of latent root and vector methods used in
661 multivariate analysis. *Biometrika* **53** (1966).

662 62 Torgeson, W. S. *Theory and Methods of Scaling*. (Wiley 1958).

663 63 Team, R. C. (R Foundation for Statistical Computing, Vienna, Austria, 2013).

664 64 Gupta, N. & Pevzner, P. A. False discovery rates of protein identifications: a strike
665 against the two-peptide rule. *Journal of proteome research* **8**, 4173-4181,
666 doi:10.1021/pr9004794 (2009).

667
668
669

670 **Figures legends**

671

672 **Fig. 1** Cell morphology of the methyl-reducing methanogens from hypersaline soda (strain
673 AMET1, **a-d**) and salt (strain HMET1, **e-f**) lakes. **a** - phase contrast image; **b** and **e** - total
674 electron microscopy images; **c-d** and **f** - electron microscopy images of thin sectioned cells. N
675 - nucleoid, PHA? - a possible PHA storage granule; CPM - cytoplasmic membrane; ICPM -
676 cell membrane invaginations; CW - cell wall.

677

678 **Fig. 2** Growth and activity of methyl-reducing methanogens from hypersaline soda lakes. **a** -
679 growth dynamics of strain AMET1 with MeOH+formate at 4 M total Na⁺, pH 9.5 and 50°C (
680 Y_{max}=1.5 mg protein/mM MeOH; μ_{max}=0.012-0.015 h⁻¹). **b** - methanogenic activity of washed
681 cells of strain AMET1 grown with MeOH+formate (at 4 M total Na⁺, pH 9.5 and 48°C) with
682 various methylated *e*-acceptors. **c** - influence of temperature on growth and activity of washed
683 cells of various AMET strains at 4 M total Na⁺, pH 9.5 with MeOH+formate as substrate. **d** -
684 influence of pH at 4 M Na⁺ on growth and activity of washed cells of strain AMET1 at 48°C
685 with MeOH+formate as substrate. **e** - influence of salinity at pH 9.5 on growth and activity of
686 washed cells of strain AMET1 with MeOH+formate as substrate. In all experiments, 100 μM
687 hydrotroilite (FeS x nH₂O) was added. Neither growth nor activity were observed with a
688 single substrate (i.e. methylated compounds, H₂ or formate alone). VCH₄ is a rate of methane
689 formation, normalized either per culture volume in growth experiments or per biomass in cell
690 suspension experiments. The results represent mean values from 2 parallel experiments in **2a**,
691 **2b** and **2d**, and from a single experiment in **2c** and **2e**.

692

693 **Fig. 3 Effect of hydrotroilite (FeS x nH₂O) on growth and methanogenic activity of**
694 **washed and exhausted cells of the AMET1 strain**

695 Growth and incubation conditions: 4 M total Na⁺, pH 9.8, 48°C. Substrate: 50 mM
696 CH₃OH+50 mM formate. The culture was grown in the presence of sterile sand. The FeS-
697 exhausted, washed cells were obtained by prolonged incubation with substrates without
698 addition of FeS followed by washing and resuspension in a fresh buffer. The results represent
699 mean values from 3 parallel experiments.

700

701 **Fig. 4 Phylogenetic analysis of "Methanonatronarchaeia" (AMET1 and HMET1)**

702 The tree represents a phylogeny of archaea based on an alignment of concatenated ribosomal
703 proteins. Methanogen clades are shown in blue and *Halobacteriales* in orange. The inferred

704 methanogenic branches are highlighted in blue, the inferred loss of methanogenesis is
705 indicated by dashed red branches. The arrow indicates the likely archaeal root. All branches
706 are supported at 100% level. The original tree is available in **Supplementary Data 1**.

707

708 **Fig. 5 Comparative genomic analysis and reconstruction of gene losses and gains**

709 **a.** Reconstruction of gene loss and gain along in "Methanonatronarchaeia" (AMET1 and
710 HMET1) and *Halobacteriales*. Light blue: arCOG complement; green: gains; dark blue:
711 losses.

712 **b.** arCOG composition of AMET1 and HMET1.

713 **c.** Distribution of the differences in the arCOG composition of AMET1 and HMET1 by
714 functional categories. For each category, the number of arCOGs unique to AMET1 and
715 HMET1 is indicated. The functional classification of the COGs is described at
716 <ftp://ftp.ncbi.nih.gov/pub/wolf/COGs/arCOG/funclass.tab>

717 **d.** Multidimensional scaling analysis of isoelectric point distributions. Orange: *Halobacteria*;
718 green: halophilic archaea and bacteria; blue: other archaea and bacteria.

719 **e.** Multidimensional scaling analysis of genes enriched in methanogens.

720

721 **Fig. 6 Reconstruction of the central metabolic pathways shared by**
722 **"Methanonatronarchaeia"**

723 The main methyl-reducing pathway is shown by thick magenta arrows. Metabolically fixed
724 low molecular weight compounds are shown in green. Either gene name or respective arCOG
725 number is shown for each reaction and shown in red (details are available at **Supplementary**
726 **Table 3**). Final biosynthetic products are shown as follows: light blue for amino acids, pale
727 yellow for nucleotides, brown for lipid components, pink for cofactors. Abbreviations: MF,
728 methanofuran; H4MPT, tetrahydromethanopterin; CoM, coenzyme M, CoB – coenzyme B,
729 CoA – coenzyme A.

730 **Table 1. Summary statistics for the AMET1 and HMET1 genomes.**

731

	AMET1	HMET1
Number of contigs	8	4
Total length (base pairs)	1513137	2141311
Number of coding sequences	1514	2168
GC content	38%	35%
rRNAs	5S, 16S, 23S	5S, 16S, 23S
tRNAs (for different amino acids including pyrrolysine)	31 (21)	37 (21)
Proteins assigned to arCOGs	88%	79%
Completeness based on archaeal core arCOGs	99% [#]	99% [#]
CRISPR arrays	0	4
CRISPR-cas system subtypes	-	I-D, III-B
Transposon-related genes	4 [*]	121 [*]
Integrated elements (His2-like viruses)	3	2

732 * - Some are probably pseudogenes; # - based on 218 core arCOGs

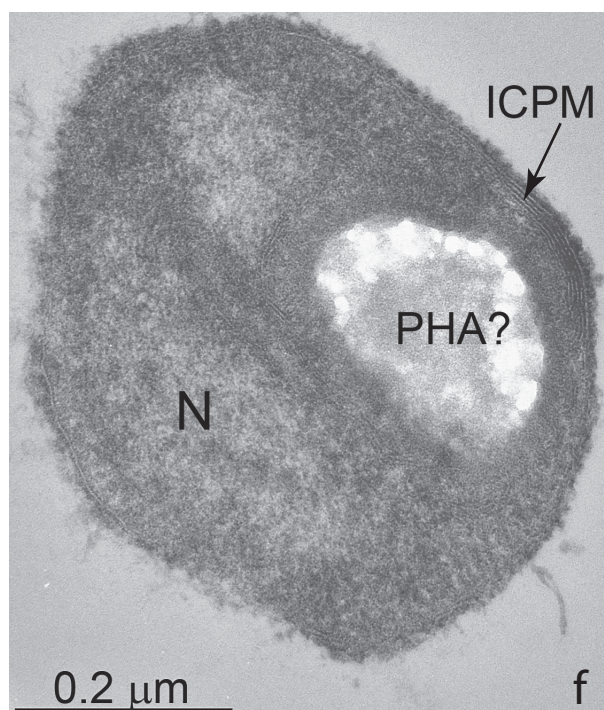
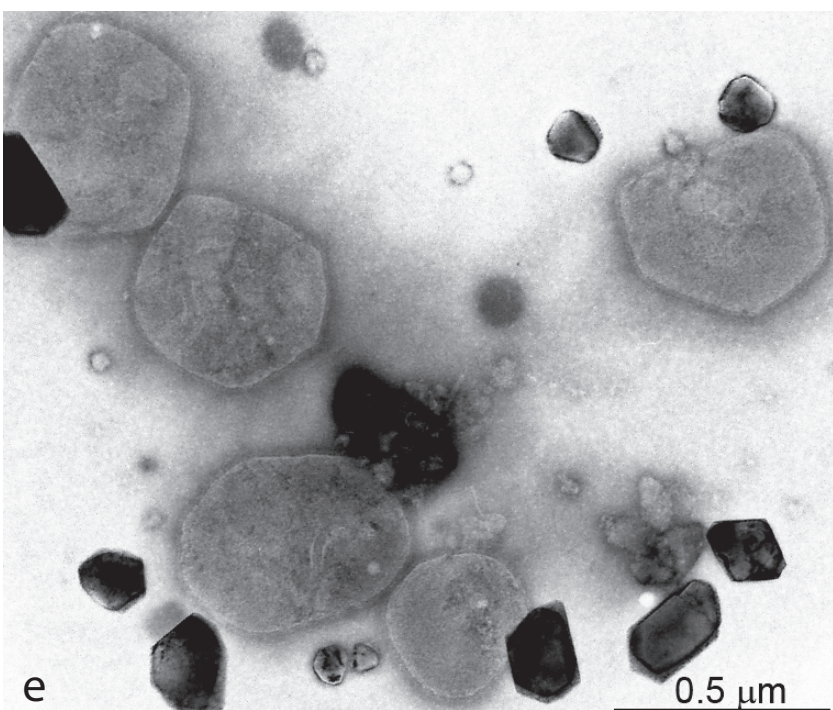
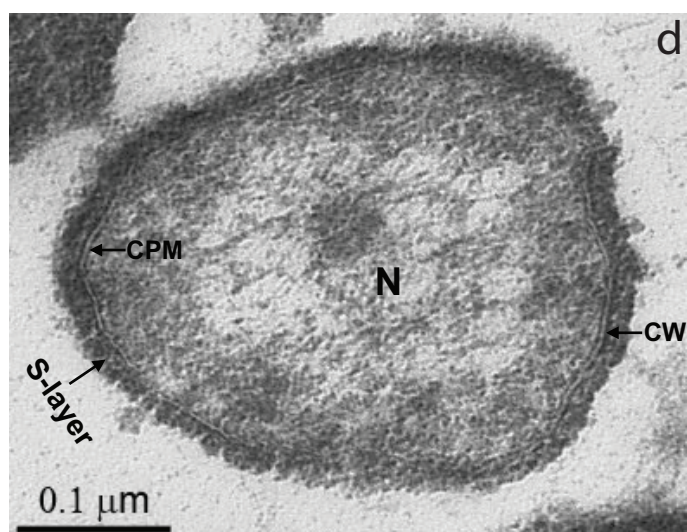
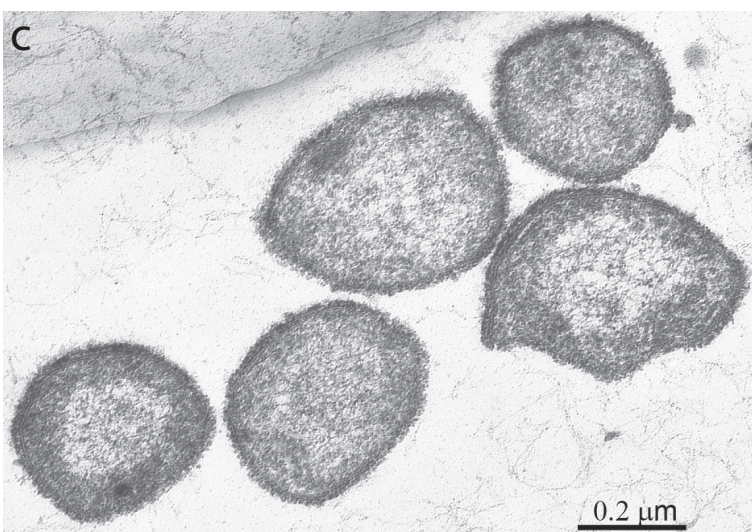
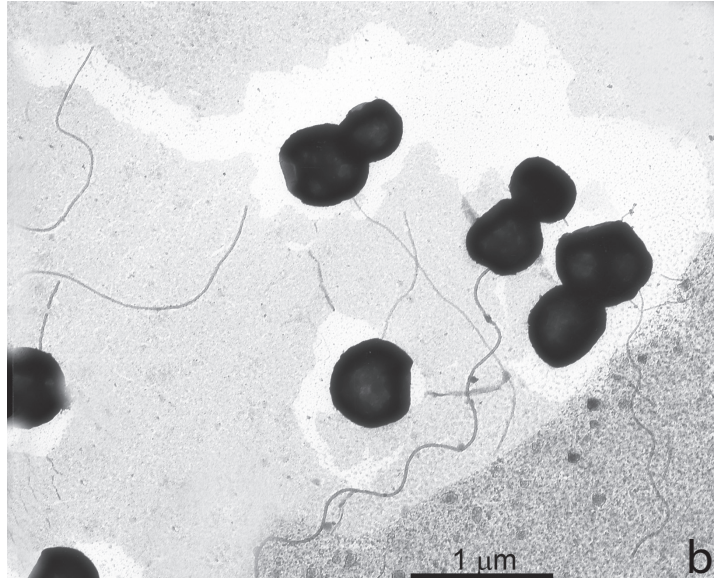
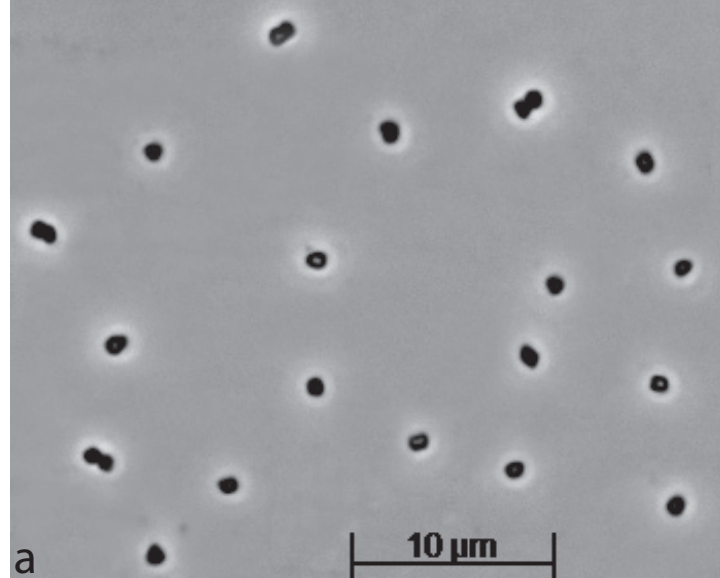


Fig. 1

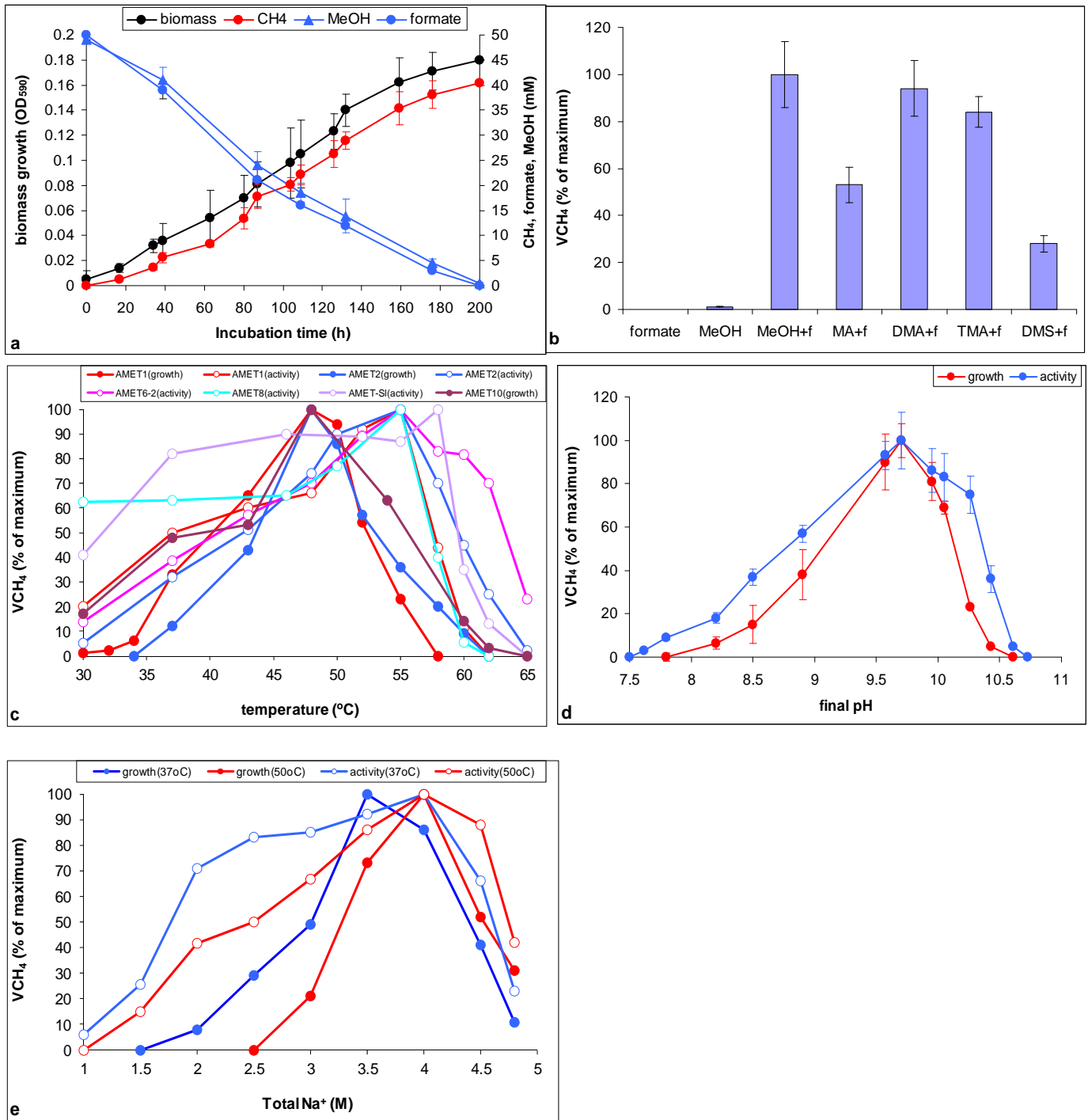


Fig.2

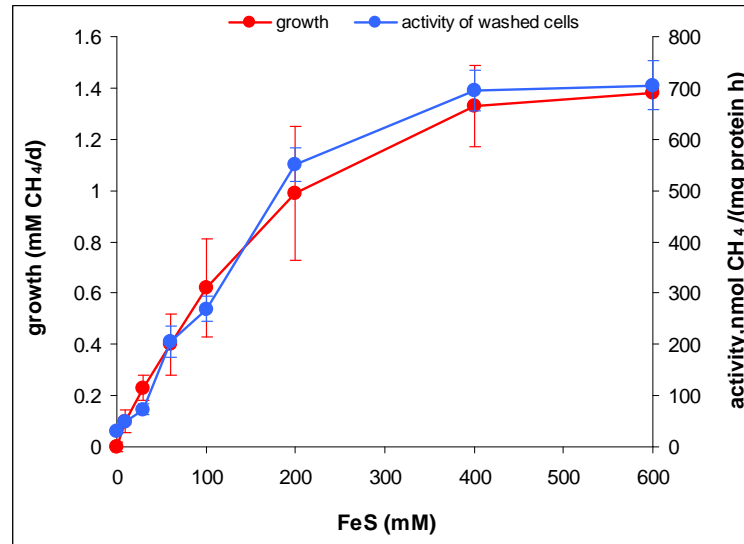
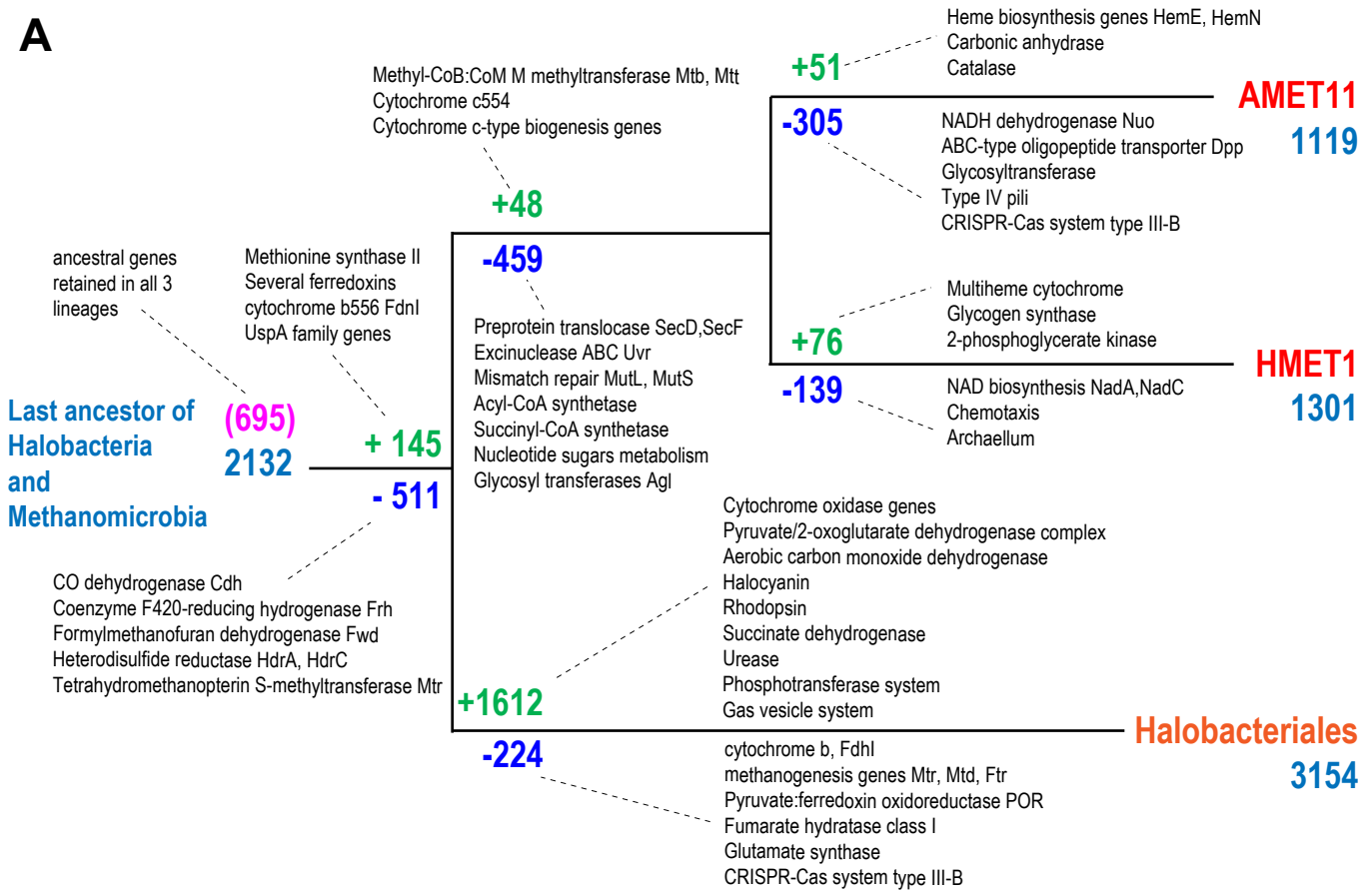
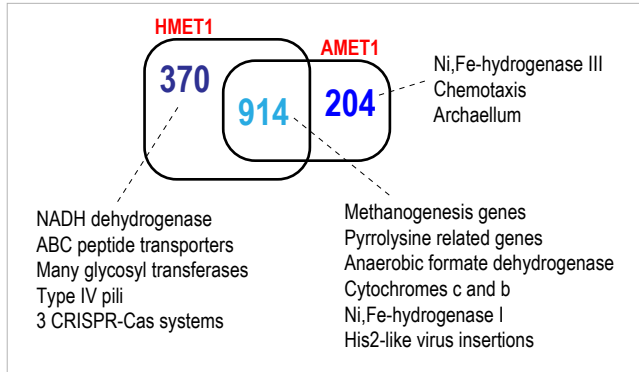
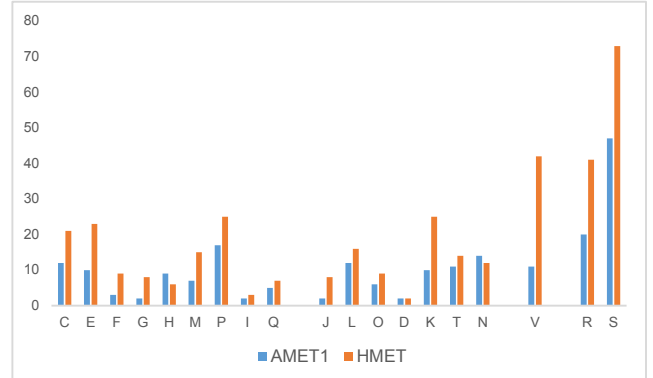
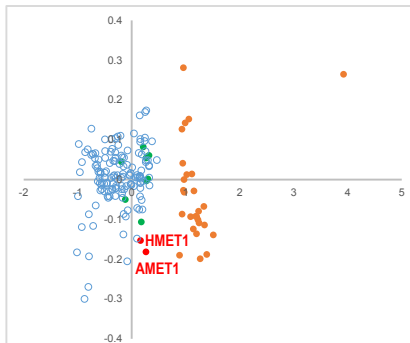
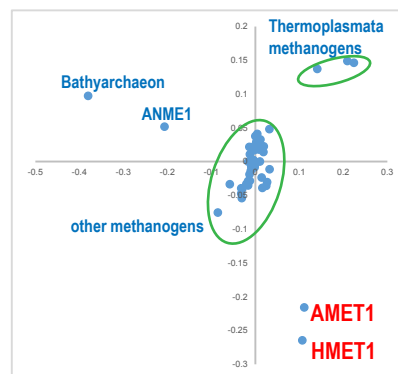


Fig.3

A**B****C****D****E****Fig.5 Comparative genomic analysis and reconstruction of losses and gains**

a. Reconstruction of gene loss and gain along in "Methanonatronarchaeia" (AMET1 and HMET1) and Halobacteriales.

Light blue: arCOG complement; green: gains; dark blue: losses. b. arCOG composition of AMET1 and HMET1. c. Distribution of arCOGs in AMET1 and HMET1

by COG functional categories. COG functional groups are described at [ftp://ftp.ncbi.nih.gov/pub/wolf/COGs/arCOG/funclass.tab](http://ftp.ncbi.nih.gov/pub/wolf/COGs/arCOG/funclass.tab) d. Multidimensional scaling

analysis of isoelectric point distributions. Orange: Halobacteria; green: halophilic archaea and bacteria; blue: other archaea and bacteria e. Multidimensional scaling analysis of genes enriched in methanogens

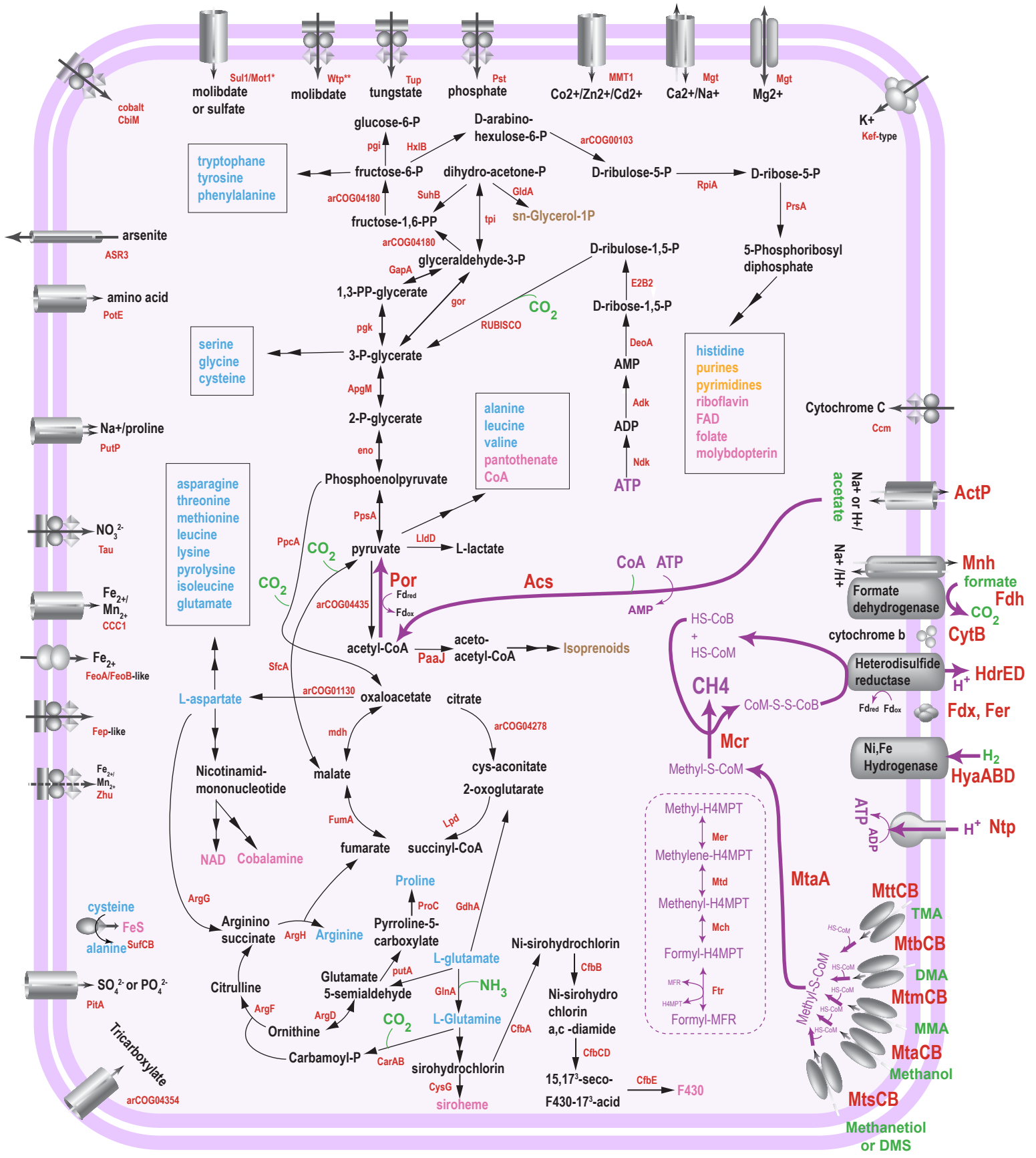


Fig.6. Reconstruction of the central metabolic pathways shared by "Methanonatronarchaeia"

The main mixotrophic pathways are shown by thick magenta arrows. Metabolically fixed low molecular weight compounds are shown in green. Either gene name or respective arCOG number is shown for each reaction and shown in red (details are available at Supplementary Table S3). Final biosynthetic products are shown as follows: light blue for amino acids, pale yellow for nucleotides, brown for lipid components, pink for cofactors. Abbreviations: MF, methanofuran; H4MPT, tetrahydromethanopterin; CoM, coenzyme M, CoB – coenzyme B, CoA – coenzyme A.